

Enhanced piezoelectricity around the tetragonal/orthorhombic morphotropic phase boundary in $(\text{Na,K})\text{NbO}_3\text{-ATiO}_3$ solid solutions

R. Wang · R.-J. Xie · K. Hanada · K. Matsusaki ·
H. Kawanaka · H. Bando · T. Sekiya · M. Itoh

Published online: 12 May 2007
© Springer Science + Business Media, LLC 2007

Abstract The high density perovskite titanates-modified potassium–sodium niobate solid solutions $(1-x)(\text{Na}_{0.5}\text{K}_{0.5})\text{NbO}_3\text{-xBaTiO}_3$ and $(1-x)(\text{Na}_{0.5}\text{K}_{0.5})\text{NbO}_3\text{-xSrTiO}_3$ have been prepared by the solid state reaction method. The phase diagram summarized from the dielectric property measurement reveals that there exists a tetragonal/orthorhombic morphotropic phase boundary for both the solid solutions. The piezoelectric properties show enhanced behavior at around the tetragonal/orthorhombic morphotropic phase boundary. It is believed that the origin for the high piezoelectric performance $(\text{Na,K})\text{NbO}_3$ -based lead-free piezoelectric ceramics is the same as that for the lead zinc niobate-lead titanate solid solution.

Keywords Morphotropic phase boundary ·
Lead-free piezoelectric · Niobate · Perovskite

1 Introduction

The morphotropic phase boundary (MPB) in lead-containing solid solutions such as $\text{Pb}(\text{Zr}_{1-x}\text{Ti}_x)\text{O}_3$ (PZT), $(1-x)\text{Pb}(\text{Mg}_{1/3}\text{Nb}_{2/3})\text{O}_3\text{-xPbTiO}_3$ (PMN-PT), and $(1-x)\text{Pb}(\text{Zn}_{1/3}\text{Nb}_{2/3})\text{O}_3\text{-xPbTiO}_3$ (PZN-PT), plays a special role. A sample with its composition around the MPB shows excellent dielectric/piezoelectric properties. It was believed that the MPBs in PZT, PMN-PT, and PZN-PT separate a tetragonal and a rhombohedral structure. However, recent research has revealed that there exists a low symmetric phase between the tetragonal and the rhombohedral phases. The low symmetric phase is a monoclinic phase for the PZT and the PMN-PT, and an orthorhombic phase for the PZN-PT [1–3]. Thus, the real MPB in the lead-containing solid solutions is a phase boundary between a monoclinic (orthorhombic) and a tetragonal structure.

In developing high-performance lead-free piezoelectric materials, searching for MPB has long been considered as an effective method. However, most of the research has been contributed to searching for the tetragonal/rhombohedral MPB. In this paper, we report our research on searching for the tetragonal/orthorhombic MPB in the perovskite titanates-modified potassium–sodium niobate.

2 Experimental procedure

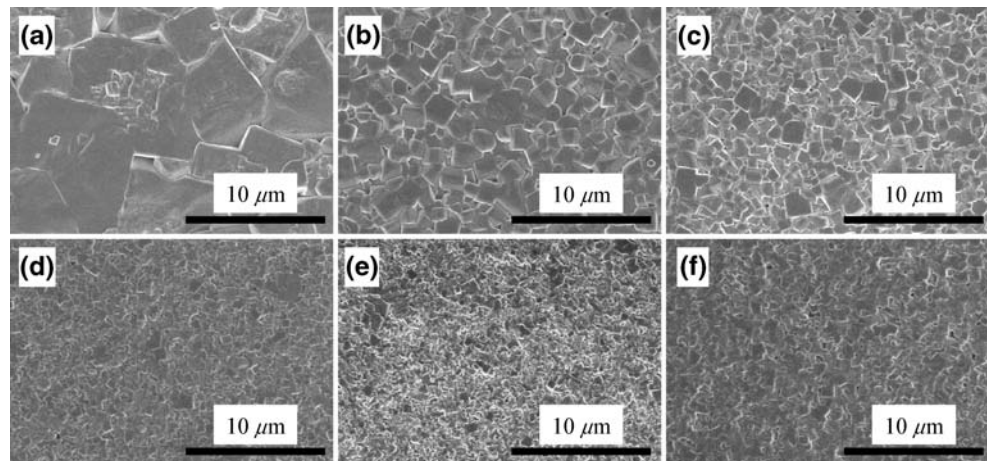
$(1-x)(\text{Na}_{0.5}\text{K}_{0.5})\text{NbO}_3\text{-xBaTiO}_3$ (NKN-BT) and $(1-x)(\text{Na}_{0.5}\text{K}_{0.5})\text{NbO}_3\text{-xSrTiO}_3$ (NKN-ST) samples were prepared by the conventional solid state reaction method. Raw materials, K_2CO_3 (3N), Na_2CO_3 (3N), BaCO_3 (3N), SrCO_3 (4N), TiO_2 (3N) and Nb_2O_5 (4N), were mixed in stoichiometric proportions and calcined at 950 °C for

R. Wang (✉) · K. Hanada · K. Matsusaki · H. Kawanaka ·
H. Bando · T. Sekiya
National Institute of Advanced Industrial Science and Technology,
Tsukuba Central 2, 1-1-1 Umezono,
Tsukuba 305-8568, Japan
e-mail: rp-wang@aist.go.jp

R.-J. Xie
National Institute for Materials Science,
1-1 Namiki,
Tsukuba 305-0044, Japan

M. Itoh
Tokyo Institute of Technology,
4259 Nagatsuta, Midori,
Yokohama 226-8503, Japan

Fig. 1 Microstructure for $(1-x)$ $(\text{Na}_{0.5}\text{K}_{0.5})\text{NbO}_3-x\text{SrTiO}_3$ solid solution with $x=0.01$ (a), 0.02 (b), 0.03 (c), 0.05 (d), 0.08 (e), and 0.10 (f)



2–10 h. The resultant powder was checked by powder X-ray diffraction (Philips X'Pert X-ray diffractometer) to be of a single phase. In order to obtain dense samples, the spark-plasma-sintering (SPS) method was used. SPS is a process in which materials are sintered using microscopic electrical discharge between particles under high sintering pressure [4–6]. SPS is usually used to produce dense metal and engineering ceramics, and only recently is being used to densify dielectric materials [7–11]. SPS is characterized by its high heating/cooling rates and the short sintering period (several minutes) and is advantageous in controlling the microstructures of samples.

About 3 g of calcined powder was charged into a graphite die of 15 mm diameter and then a pressure of 30–60 MPa was applied. The sintering temperature was about 1000–1100 °C and the soaking time was 2–5 min. The resultant pellets, which were black in color due to the use of the graphite die and sintered under reduced atmosphere, were then annealed at 950–1100 °C under the atmosphere of $(\text{Na}_{0.5}\text{K}_{0.5})\text{NbO}_3$ to prevent the evaporation of sodium and potassium. The microstructure of the samples was observed by scanning electron microscopy (Hitachi, S-4500).

For the dielectric and the piezoelectric measurements, silver paste, burnt onto the samples at 600 °C, was used as electrodes. The dielectric constant was measured using an Agilent 4194A impedance analyzer over a temperature range of $30 \leq T \leq 500$ °C. For the piezoelectric measurement, samples were poled at ~130–150 °C for 30 min under an electric field of 20–40 kV/cm. The electromechanical coupling coefficient k_p was measured by the resonance anti-resonance method with an impedance analyzer (Agilent, HP4194A). The piezoelectric d_{33} constants were measured by using a piezo- d_{33} meter (APC International, Ltd, Wide-Range d_{33} Tester).

3 Results and discussion

The microstructures of NKN-ST samples with $x=0.01$, 0.02, 0.03, 0.05, 0.08, and 0.10 observed by the scanning electronic microscopy (SEM) are shown in Fig. 1. It is obvious that for all the samples, grains are closely packed and few pores exist. Except for the sample with $x=0.01$, the grain size is fairly homogenous. The average grain size is about 1.5 μm , 0.5 μm and 0.25 μm for the samples with $x=0.03$, 0.05, and 0.10, respectively. That is, with increasing the SrTiO_3 content x , grain size tends to decrease. The same trend is also observed in the NKN-BT solid solution. The relative density, estimated from the weight and the size of the samples, is higher than 96% of the theoretical density for all the samples.

The temperature dependence of the dielectric constant at 10 kHz is shown in Fig. 2. Above the room temperature, the $x=0$ sample, $(\text{Na}_{0.5}\text{K}_{0.5})\text{NbO}_3$, shows two dielectric constant peaks at around 420 and 210 °C, respectively. The two peaks correspondent to two phase transitions: cubic-tetragonal (C–T) and tetragonal–orthorhombic (T–O), respectively. At the room temperature, $(\text{Na}_{0.5}\text{K}_{0.5})\text{NbO}_3$ possesses an orthorhombic structure. On increasing x , both the C–T transition temperature and the T–O transition temperature shift to lower values. For the samples with $x \geq 0.05$, the T–O transition temperature are lower than the room temperature. Accompanying with the lowering of the phase transition temperatures, both phase transitions become more and more diffused. These behaviours are very similar to the $(1-x)(\text{Na}_{0.5}\text{K}_{0.5})\text{NbO}_3-x\text{PbTiO}_3$ (NKN-PT) samples [10, 11].

The phase diagrams of NKN-BT and NKN-ST summarized from the dielectric constant measurements (Fig. 2) and that of NKN-PT from our previous paper [11] are

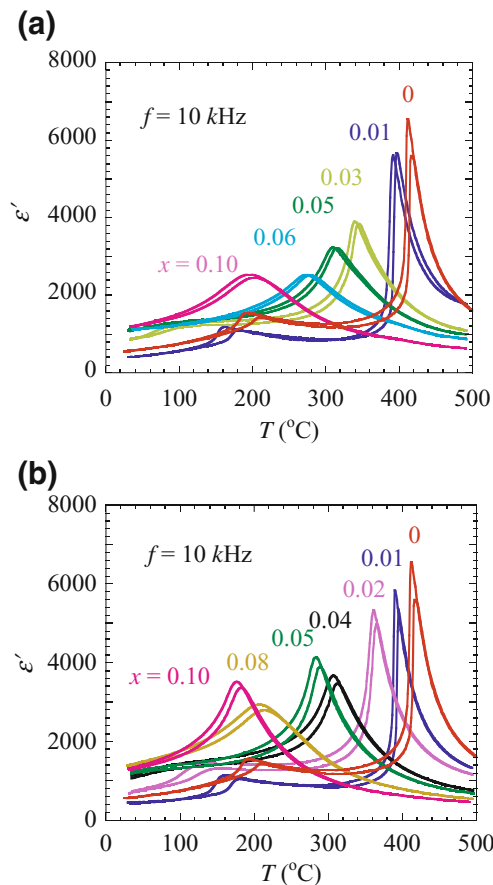


Fig. 2 (a) Temperature dependence of the dielectric constant for $(1-x)(\text{Na}_{0.5}\text{K}_{0.5})\text{NbO}_3-x\text{BaTiO}_3$ solid solution. (b) Temperature dependence of the dielectric constant for $(1-x)(\text{Na}_{0.5}\text{K}_{0.5})\text{NbO}_3-x\text{SrTiO}_3$ solid solution

compared in Fig. 3. The phase diagram for the three solid solutions was very similar. Upon introducing a small amount of $A\text{TiO}_3$ ($A=\text{Pb}, \text{Ba},$ and Sr), both the C–T and the T–O phase transition temperatures rapidly decreased. The transition temperature of C–T, T_{c1} , is different for different A ($A=\text{Pb}, \text{Ba}, \text{Sr}$). However, the transition

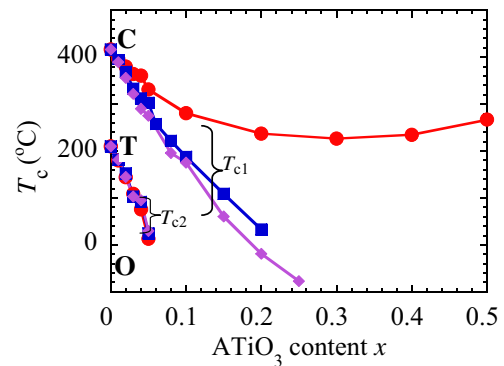


Fig. 3 Phase diagram for $(1-x)(\text{Na}_{0.5}\text{K}_{0.5})\text{NbO}_3-x\text{BaTiO}_3$ and $(1-x)(\text{Na}_{0.5}\text{K}_{0.5})\text{NbO}_3-x\text{SrTiO}_3$, solid solutions. The data for $(1-x)(\text{Na}_{0.5}\text{K}_{0.5})\text{NbO}_3-x\text{PbTiO}_3$ solid solution is plotted for comparison. With decreasing temperature, the structure changes from cubic(C) to tetragonal(T), and to orthorhombic(O), respectively

temperature of T–O, T_{c2} , is almost independent of A ($A=\text{Pb}, \text{Ba}, \text{Sr}$). The tetragonal/orthorhombic MPB is found around $x\sim 0.05$, where dT_2/dx is about -3400 $^\circ\text{C}/\text{mol}$. This value is much larger than the dT_c/dx for usual solid solutions (e.g. -400 $^\circ\text{C}/\text{mol}$ for $(\text{Ba},\text{Sr})\text{TiO}_3$) and is the same order as the $dT_c/dx\sim -5800$ $^\circ\text{C}/\text{mol}$ for PZT ceramics near MPB.

The piezoelectric properties of the NKN-BT and the NKN-ST solid solutions are listed in the Table 1. The sample with $x=0$ was well poled. The radial electro-mechanical coupling coefficient k_p was 33% and the piezoelectric constant d_{33} was 122 pC/N. Both k_p and d_{33} tend to increase with increasing x . The highest k_p and d_{33} values were 34% and 150 pC/N for NKN-BT at $x=0.06$ and 37% and 195 pC/N for NKN-ST at $x=0.05$, respectively. That is for both NKN-BT and NKN-ST, the piezoelectric properties maximize around the tetragonal/orthorhombic MPB. Both k_p and d_{33} rapidly decreased when x was beyond 0.05–0.06.

More detailed measurements have shown that the space group for the tetragonal and the orthorhombic phases of the

Table 1 Piezoelectric properties of the NKN-BT and the NKN-ST solid solutions.

| x | NKN-BT | | | | NKN-ST | | | |
|------|-------------------------------|-----------|-----------------|--------------------|-------------------------------|-----------|-----------------|--------------------|
| | T_{c1} ($^\circ\text{C}$) | k_p (%) | d_{33} (pC/N) | Phase ($^\circ$) | T_{c1} ($^\circ\text{C}$) | k_p (%) | d_{33} (pC/N) | phase ($^\circ$) |
| 0 | 417 | 33 | 122 | 73 | 417 | 33 | 122 | 73 |
| 0.01 | 397 | 34 | 112 | 68 | 397 | 31 | 110 | 59 |
| 0.02 | 369 | 23 | 76 | 31 | 374 | 32 | 133 | 72 |
| 0.03 | 344 | 33 | 133 | 71 | 335 | 27 | 137 | 58 |
| 0.04 | 315 | 31 | 144 | 64 | 313 | 35 | 155 | 70 |
| 0.05 | 307 | – | – | – | 289 | 37 | 195 | 75 |
| 0.06 | 279 | 34 | 150 | 64 | – | – | – | – |
| 0.08 | – | – | – | – | 215 | 23 | 112 | 49 |
| 0.10 | 204 | 15 | 55 | –20 | 182 | 23 | 104 | 47 |

tetragonal/orthorhombic MPB in the NKN-PT, NKN-BT and the NKN-ST solid solutions are the same as that in the PZN-PT solid solution [12]. Thus, it is suggested that the mechanism responsible for the high piezoelectric performance in the PZN-PT solid solution and that for the (Na,K)NbO₃-based lead-free piezoelectric ceramics is the same.

4 Summary

By introducing the perovskite titanates BaTiO₃ and SrTiO₃ to potassium–sodium niobate, a tetragonal/orthorhombic MPB has been formed for both the solid solutions. The values of k_p and d_{33} maximize at around the tetragonal/orthorhombic morphotropic phase boundary. It is believed that the origin for the high piezoelectric performance (Na, K)NbO₃-based lead-free piezoelectric ceramics is the same as that for the lead zinc niobate-lead titanate solid solution. However, the conclusion is to be supported by the crystal structure analysis.

Acknowledgment Financial support by the Japan Society for the Promotion of Science (No. 16560621) is acknowledged.

References

1. B. Noheda, D.E. Cox, G. Shirane, R. Guo, B. Jones, L.E. Cross, *Phys. Rev. B* **63**, 014103 (2000)
2. D. La-Orauttapong, B. Noheda, Z.-G. Ye, P.M. Gehring, J. Toulouse, D.E. Cox, G. Shirane, *Phys. Rev. B* **65**, 144101 (2002)
3. B. Noheda, D.E. Cox, G. Shirane, J. Gao, Z.-G. Ye, *Phys. Rev. B* **66**, 054104 (2002)
4. M. Tokita, *J. Soc. Powder Technol. Jpn.* **30**, 790 (1993)
5. I. Kondoh, T. Tanaka, N. Tamari, *J. Ceram. Soc. Jpn. (Yogyo Kyokaishi)* **102**, 505 (1994)
6. N. Tamari, T. Tanaka, K. Tanaka, I. Kondoh, M. Kawahara, M. Tokita, *J. Ceram. Soc. Jpn. (Yogyo Kyokaishi)* **103**, 740 (1995)
7. T. Takeuchi, E. Betourne, M. Tabuchi, H. Kageyama, Y. Kobayashi, A. Coats, F. Morrison, D.C. Sinclair, A.R. West, *J. Mater. Sci.* **34**, 917 (1999)
8. T. Takeuchi, M. Tabuchi, I. Kondoh, N. Tamari, H. Kageyama, *J. Am. Ceram. Soc.* **83**, 541 (2000)
9. J.-K. Park, U.-J. Chung, N.-M. Hwang, D.-Y. Kim, *J. Am. Ceram. Soc.* **84**, 3057 (2001)
10. R. Wang, R.-J. Xie, T. Sekiya, Y. Shimojo, Y. Akimune, N. Hirotsuki, M. Itoh, *Ferroelectrics* **286**, 93 (2003)
11. R. Wang, R.-J. Xie, T. Sekiya, Y. Shimojo, Y. Akimune, N. Hirotsuki, M. Itoh, *Jpn. J. Appl. Phys.* **41**, 7119 (2002)
12. R. Wang, R.-J. Xie, K. Hanada, K. Matsusaki, H. Bando, M. Itoh, *Phys. Status Solidi* **202**, R57 (2005)